Numerical analysis on three dimensional flow and bed topography in a compound meandering channel

S. Fukuoka
Department of Civil and Environmental Engineering, Hiroshima University, JAPAN

A. Watanabe
Department of Civil and Environmental Engineering, Hiroshima University, JAPAN

ABSTRACT: For the evaluation of the effects of relative depth, sinuosity of the channel and roughness over the structure of flows and river bed topography in a compound meandering channel, a three dimensional numerical model was developed. In this model, the spectral method was used to compute the distribution of flow, water surface elevation, pressure intensity and bed height. This numerical model can evaluate and reproduce accurately the features of the flow field and bed topography observed in laboratory. This paper examined the effects of assuming the hydrostatic pressure approximation on the flow and the bed variation. It was considered that the use of a hydrodynamic pressure model is necessary for evaluating the deformation in a compound meandering channel with high relative depth values. The numerical analysis has shown the importance of secondary flow structures in the formation of the bed features.

1 INTRODUCTION

It was shown that flow field and bed profile in a compound meandering channel differ greatly from those of bankful flow when the depth over the flood plain is large to the bankful depth in the main channel, by Ashida et al. (1989, 1990), Kinoshita (1988), and Mori (1986a, 1986b). Among these differences first, the maximum velocity filament in the main channel runs near the inner banks; regarding the secondary flows, the rotation is reversed from that observed in bankful flows (Fukuoka et al., 1996 and Muto, 1997). These changes in the flow fields are accompanied by the cessation of scouring at outer bank bed and by the scouring near the inner bank (Fukuoka et al. 1997).

It is generally believed that these flow characteristics are depending on the sinuosity and the phase difference between the main channel alignment and the levee alignment, the relative depth, the ratio of roughness and width between flood channel and main channel, and so on. The effects of relative depth and sinuosity were shown by means of the large-scale hydraulic experiments performed by Fukuoka et al. (1997a, 1997b) and the flow velocity distributions calculated from actual aerial surveying photographs (Fukuoka et al., 1997c).

It has been shown that the geometrical and hydraulic conditions affect dramatically the features of the flow structure in a compound meandering channel, therefore numerical analysis should be used to compute flow variables and bed evolution. Therefore, efforts are made to develop three-dimensional numerical models that might represent compound meandering flows. Jin et al. (1996) developed a two-layer model and then showed that a three dimensional statistical turbulence model is applicable for the flows of low relative depth. The authors developed a numerical model that uses the spectral method to express three dimensional flows in compound meandering channels with fixed bed (Fukuoka et al., 1998) and it is able to express the changes in the structure of flow due to the changes in the relative depth.

This paper describes the numerical analysis model incorporating bed variations into a 3-D flow model (Fukuoka et al., 1998 and Watanabe et al., 1999) developed by the authors, and discusses its suitability for flow and bed

variation against the change in the relative depth. In this paper, two flow models with and without a assumption of hydrostatic pressure mode are used to examine the significance of change in pressure intensity.

2 METHOD OF ANALYSIS

2.1 Introduction of the plane curve coordinate system and σ coordinate system

Coordinate transformation is used as a simple way to incorporate the effects of the complex boundary profile into the numerical analysis. Figure 1 shows the profile of the compound channel to be analyzed, together with the coordinate system. The plane coordinate systems are transformed from rectangular ones (x, y) to curvilinear ones (ξ, η). As shown in Figure 2, the vertical coordinate system z is transformed into σ coordinate system, which is defined as

$$\begin{cases} z = z_o + (z_o - z_p)\sigma, \ (\sigma \geq 0) \\ z = z_p + (z_p - z_b)\sigma, \ (\sigma < 0) \end{cases} \quad (1)$$

where z_o, z_p and z_b represent the reference plane near the water surface, flood channel and bed heights respectively. The values σ = 1, 0, -1 represent the reference plane, flood channel and bed heights, respectively. At this time, the scale parameters relating to the vertical axis are respectively represented by using depths above and below a flood channel. If z_o and z_p are constant, the metric tensors can be evaluated from changes in the bed surface or the depth below the flood channel alone, without having to incorporate mesh movement. Thus, a coordinate system results in the following metric tensor matrix.

$$\begin{bmatrix} \xi_x & \eta_x & \sigma_x \\ \xi_y & \eta_y & \sigma_y \\ \xi_z & \eta_z & \sigma_z \end{bmatrix} = \begin{bmatrix} y_\eta / J' & -y_\xi / J' & -(z_\xi \xi_x + z_\eta \eta_x)/z_\sigma \\ -x_\eta / J' & x_\xi / J' & -(z_\xi \xi_y + z_\eta \eta_y)/z_\sigma \\ 0 & 0 & 1/z_\sigma \end{bmatrix} \quad (2)$$

$$J = J' z_\sigma, \quad J' = x_\xi y_\eta - x_\eta y_\xi \quad (3)$$

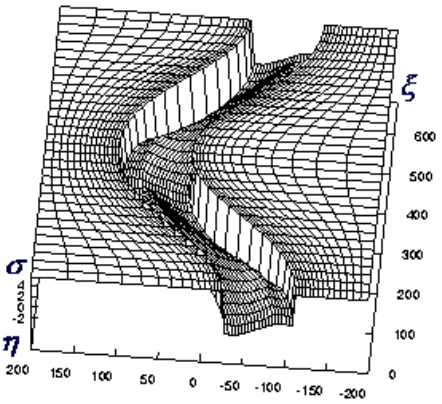

Figure 1: Coordinate system and computational domain for compound meandering channel with movable bed. (Length unit: cm)

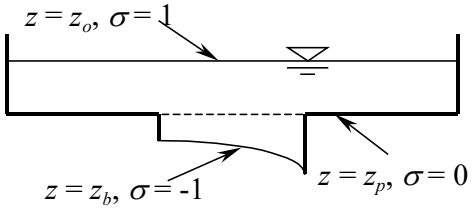

Figure 2: Definition of σ coordinate system.

Where subscripts in the coordinate system indicate the partial differentiation of that coordinate, zt represents time, and J the Jacobian. Contravariant flow velocity is represented in the curvilinear coordinate system as follows:

$$\begin{cases} U = \xi_x u + \xi_y v \\ V = \eta_x u + \eta_y v \\ W = \sigma_z W' = \sigma_z (\sigma_x' u + \sigma_y' v + w) \end{cases} \quad (4)$$

Where u = x-direction flow velocity; v = y-direction flow velocity; w = z-direction flow velocity; U = ξ-direction contra-variant flow velocity; V = η-direction contra-variant flow velocity and W = σ-direction contra-variant flow velocity. In Equation 4, σ_x' and σ_y' represent the quantities defined by $\sigma_x = \sigma_x' \sigma_z$ and $\sigma_y = \sigma_y' \sigma_z$.

2.2 Basic equations of the flow

When the coordinate system is introduced as described above, the equation of motion that approximates the hydrostatic pressure is expressed as follows:

$$\frac{\partial u}{\partial t}+U_j\frac{\partial u}{\partial \xi_j}=g_x-g\xi_{j,x}\frac{\partial \zeta}{\partial \xi_j}+\upsilon_T\Delta u -\frac{1}{\rho}\xi_{j,x}\frac{\partial p}{\partial \xi_j} \quad (5a)$$

$$\frac{\partial v}{\partial t}+U_j\frac{\partial v}{\partial \xi_j}=g_y-g\xi_{j,y}\frac{\partial \zeta}{\partial \xi_j}+\upsilon_T\Delta v -\frac{1}{\rho}\xi_{j,y}\frac{\partial p}{\partial \xi_j} \quad (5b)$$

$$\frac{\partial w}{\partial t}+U_j\frac{\partial w}{\partial \xi_j}=g_z-\frac{1}{\rho}\sigma_z\frac{\partial p}{\partial \sigma}+\upsilon_T\Delta v \quad (5c)$$

$$\Delta=\frac{\partial^2}{\partial x_j^2} \qquad (j=1,2,3)$$

Where g_x, g_y, g_z = gravitational acceleration in the respective directions, ζ = water level fluctuation relative to the reference surface, p = deviation pressure from the hydrostatic pressure. The eddy viscosity ν_T is expressed in the following equation using h = depth from the reference surface, z_d = height from the bottom, and u_* = bottom friction velocity.

$$\nu_T=\kappa u_* z_d(1-z_d/h) \quad (6)$$

The continuity equation is expressed as

$$\frac{\partial JU_j}{\partial \xi_j}=0 \quad (7)$$

Integration of Equation 7 from the bed level (σ =-1) to the water surface ($z=z_o+\zeta$) produces Equation 8, when ζ indicates water level fluctuation:

$$J'\frac{\partial \zeta}{\partial t}+\frac{\partial}{\partial \xi_k}\int_{-1}^{\sigma(z_o+\zeta)}J'z_\sigma U_k d\sigma=0 \quad (k=1,2) \quad (8)$$

The kinematic boundary conditions are used to assign the contra-variant flow velocity W' in the σ -direction at the water surface is expressed by Equation 9:

$$\frac{\partial \zeta}{\partial t}+U_k\frac{\partial \zeta}{\partial \xi_k}=W', \quad (z=z_o+\zeta) \quad (9)$$

In the analysis without the assumption of hydrostatic pressure (model I), the deviation pressure p is solved quickly in the spectral space by using SMAC method for Equation 5 and 7 (Fukuoka et al., 1998). On the contrary in the model with the assumption of hydrostatic pressure (model II), p = 0 and Equation 5c is not used in model I. The distribution of vertical velocity w is given by the integral of Equation 7 from the bottom.

2.3 Basic equations of the bed deformation

The bed variation is expressed by using the sediment continuity equation as follows:

$$J'\frac{\partial z_b}{\partial t}+\frac{1}{1-\lambda}\left(\frac{\partial J'q_{B\xi}}{\partial \xi}+\frac{\partial J'q_{B\eta}}{\partial \eta}\right)=0 \quad (10)$$

Where ($q_{B\xi}$, $q_{B\eta}$) is the contra-variant sediment discharge vector as given by

$$\begin{cases} q_{B\xi}=q_B\left\{\dfrac{U_b}{\sqrt{u_{kb}^2}}-\dfrac{1}{\sqrt{\mu_s\mu_k}}\dfrac{u_{*c}}{u_*}(\xi_{1,i}\xi_{k,i}\dfrac{\partial z_b}{\partial \xi_k})\right\} \\ q_{B\eta}=q_B\left\{\dfrac{V_b}{\sqrt{u_{kb}^2}}-\dfrac{1}{\sqrt{\mu_s\mu_k}}\dfrac{u_{*c}}{u_*}(\xi_{2,i}\xi_{k,i}\dfrac{\partial z_b}{\partial \xi_k})\right\} \end{cases} \quad (i,k=1,2) \quad (11)$$

Equation 11 is obtained through the coordinate transformation of the longitudinal and transverse sediment discharge vector (Fukuoka et al., 1993). The effects of the bed gradient are incorporated in Equation 11. Here, q_B = bed load, μ_s = static friction factor, μ_k = dynamic friction factor, u_{*c} = critical friction

velocity, and the subscript b indicates the value at the bed. This analysis employs the Ashida-Michiue equation for sediment discharge calculation, and to incorporate additional tractive force and changes in critical tractive force (Fukuoka et al., 1983) due to the bed slope change.

2.4 Introduction of spectral method and formulation

Because the profile of the boundary and the flow field are changed periodically in the longitudinal direction, Fourier series expansions are applied for the plane boundary profile, the flow field and the bed profile in this direction. The spectral collocation method is employed to solve the differential equation in the longitudinal direction. For this analysis, the series is expanded from the 0th mode to the 7th mode, and 32 spectral collocation points were selected as shown in Figure 1.

For the flow field analysis, a longitudinal differentiation was calculated by differentiating in the spectral space and then the value was inverting to the spectral collocation point through inverse Fourier transformation. The convective terms in (η, σ) plane were differentiated using an upwind difference of 1st and 3rd order in the vertical and transverse direction respectively.

2.5 Boundary conditions and their method of calculation

Using the procedure outlined in section 2.4, velocities u, v, w, pressure p and water level ζ are calculated on the spectral points and then time-integrated in spectral space. The time integrals of velocity and water level are explicitly calculated with the Huen method having 2nd order accuracy in time. The bed deformation is very slow in comparison with the velocity adjustment, therefore, the time variations of bed and velocity are repeatedly calculated at separate time scales in this analysis.

The resistance at the walls is taken proportional to the square of the velocity in the vicinity, being assigned as a boundary condition for velocity. Impermeable slip-conditions are also applied at the walls. Friction velocities on the side walls and the bottom are determined by dividing velocities near the walls and the bed by the resistance coefficient respectively.

3 FLOW AND BED DEFORMATION ANALYSIS

3.1 Conditions for experimentation and calculation

The plane profile of the compound channel is shown in Figure 1, where the total width = 4.0 m; main channel width = 0.8 m; mean main channel bank height = 0.055 m; meander length = 6.8 m; and sinuosity = 1.1. There are five and two vertical calculation points below and above the flood channel height respectively.

The authors analyzed Cases 3 and 5 in the large-scale experiments by Fukuoka et al. (1997b). The experimental channel was 15 m long. The flood channel was covered with artificial turf to create the appropriate roughness and the main channel was filled with sand 0.8 mm in diameter. The slope of the channel and bed was 1/600. The resistance coefficient at the bottom was calculated by using the equivalent roughness k_s and $z_{1/2}$ using Equation 12.

$$\varphi_b = 5.75 \log(z_{1/2} / k_s) + 8.5 \qquad (12)$$

Where, $z_{1/2}$ is the height in the center, the calculation point for flow velocity, of the 1st bottom mesh. It was assumed that k_s = 2.8 cm in the flood channel. Because of the tractive force, the value of the sand diameter was used for k_s at the bottom, but it did not include the resistance due to sand wave.

Table 1. Conditions for analysis

Case	Discharge (*l*/s)	Main Channel depth (cm)	Flood Channel depth (cm)	Relative Depth Dr
3	35.9	8.0	2.5	0.31
5	63.7	10.6	5.3	0.49

Table 1 gives the conditions of numerical analysis. For this analysis, the conditions were

decided to produce a depth (i.e., relative depth) equivalent to that used in the experiment, and the resistance coefficient was fixed so that the calculated discharge would match the experimental discharge.

3.2 Bed deformation

Figures. 3 and 4 show the observed and calculated bed shape by contour lines respectively for Case 3. Figures. 5 and 6 show similar results for Case 5. In both the cases the flow proceeds from the left to the right. The observed results show the bed shape of one wave-length in the central part of channel. The calculated bed shapes are obtained from model I, without assumption of hydrostatic pressure.

Comparing Figure 5 with Figure 6, the calculated scouring occurs continuously from the inner bank to the next inner bank at the maximum curvature and the calculated result is similar to the observed one. On the other hand, The bed shape in Figures 4 does not agree with one in Figure 3. In the observed results, bed scouring occurs at the maximum curvature. In the calculated results, a scouring region spreads out from the outer bank to the inner bank and the maximum scouring occurs near the bank at the maximum curvature. This means that the observed bed shape in Dr=0.31 has the characteristics of a compound meandering flow but the calculated bed shape in Dr=0.31 has one of a single-section meandering flow.

Generally, the bed shape changes from one in a single section meandering channel to one in a compound meandering channel around where the relative depth becomes 0.3. However, this transition of bed shape is sensitive to the roughness of bed and so on. The river bed can take both shapes to this relative depth. When the effects of the secondary flow mentioned in the following section surpass the effects of the longitudinal change in the tractive force for the bed deformation, the bed shape becomes one in a compound meandering channel. The slight difference between observed and calculated results for the scouring position are due to the difference of bed roughness and the use of periodic boundary conditions for the experiment results which were not actually periodic.

3.3 Characteristics of flow field

Figures 7 and 8 show the calculated velocity vectors at below and above flood channel height respectively for Case 3. Figures 9 and 10 show similar results for Case 5. As shown in

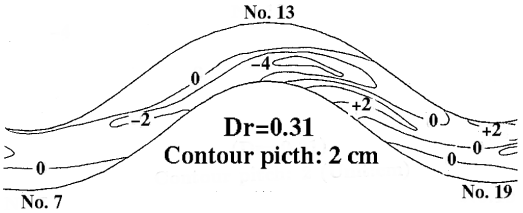

Figure 3: Bed variation contour in Case 3. (Observed results)

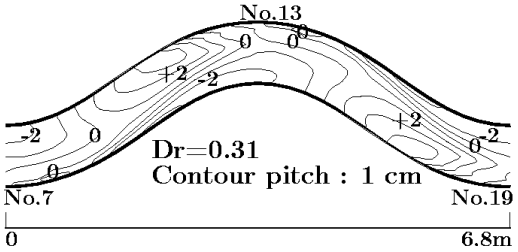

Figure 4: Bed variation contour in Case 3. (Calculated results by model I)

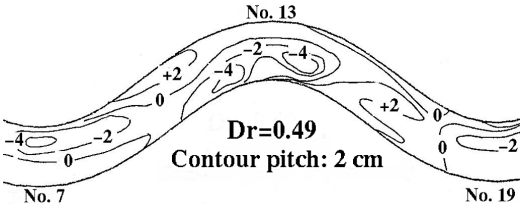

Figure 5: Bed variation contour in Case 5. (Observed results)

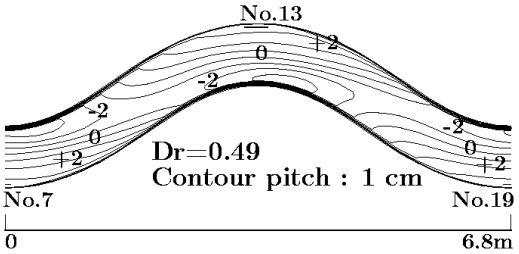

Figure 6: Bed variation contour in Case 5. (Calculated results by model I)

Figure 7, flow below flood channel height concentrates near the inflection point of outer bank and scouring occurs there.On the contrary in Figure 9, flow dose not so concentrate and the change in velocity is small. But, the flow

over bed goes towards the outer bank and bed materials move to the bank by this secondary flow. As shown in Figure 8 (Dr = 0.31), the main flow above the height of flood channel proceeds along the main channel. The velocity over the flood channel is small and the velocity changes considerably in the transverse direction.

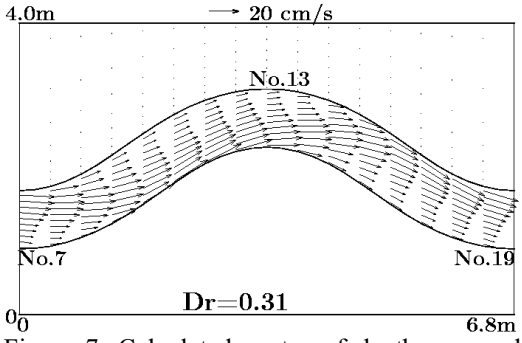

Figure 7: Calculated vector of depth-averaged velocity below flood channel height in Case 3.

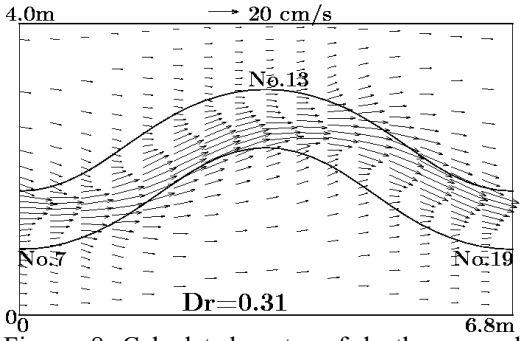

Figure. 8: Calculated vector of depth-averaged velocity above flood channel height in Case 3.

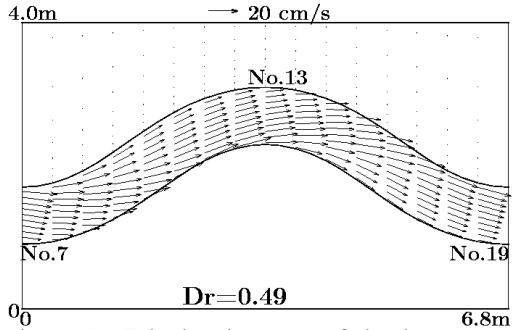

Figure 9: Calculated vector of depth-averaged velocity below flood channel height in Case 5.

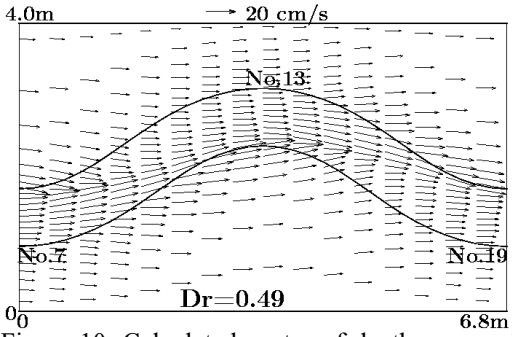

Figure 10: Calculated vector of depth-averaged velocity above flood channel height in Case 5.

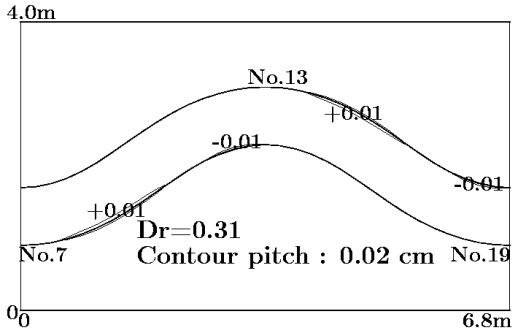

Figure 11: Calculated depth-averaged pressure deviation below flood channel height in Case 3.

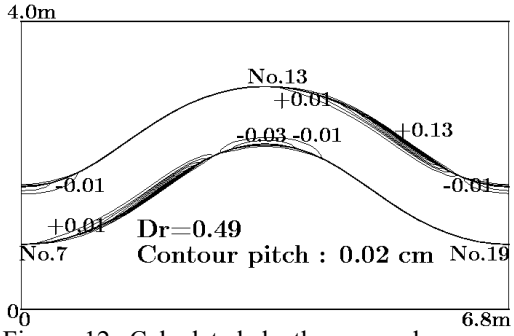

Figure 12: Calculated depth-averaged pressure deviation below flood channel height in Case 5.

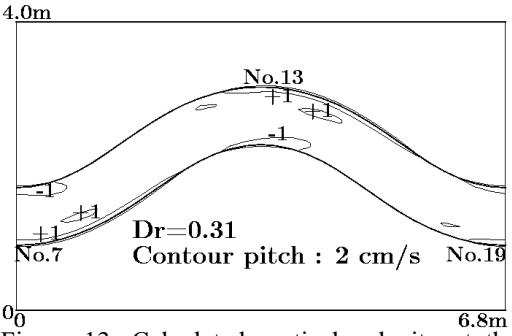

Figure 13: Calculated vertical velocity at the height of flood channel in case 3.

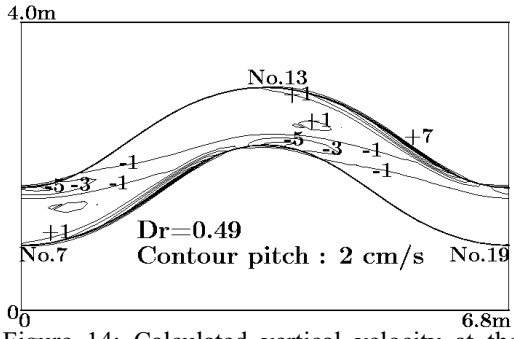

Figure 14: Calculated vertical velocity at the height of flood channel in Case 5.

But, the momentum exchange between flow in main channel and above flood channel is small, as the exchange in rate of flow is small in small relative depth. On the contrary in Figure 10, flow goes along the levee of flood channel and the velocity above flood channels is large. Comparing Figures 9 and 10, the direction of the secondary flows is reversed from one observed in a single section meandering flow.

Figures 11 and 12 show the distribution of calculated pressure deviation for case 3 and 5 respectively. When the relative depth is small, the pressure deviation in a main channel below the height of flood channel is small and pressure is almost hydrostatic condition. When the relative depth is large, however, the pressure deviation is large near the bank around the inflection point and the apex of meandering.

Figures 13 and 14 show the distribution of calculated vertical velocity at the height of flood channel for case 3 and 5 respectively. As shown in Figure 14, flow rise up near the bank around the inflection point from lower channel and goes down to lower channel around apex. These places exist where the change in the pressure intensity is large. In Figure 13, the large vertical velocity is not seen. Comparing Figures 9 and 14, we can find that the faster flow goes down into lower channel and is diverging over the bed. At the same time Figure 6 indicates that the bed scouring occurs continuously over the area where the faster flow goes down. The tractive force is larger over the area where the fast flow goes down and flow goes out of this area with bed materials. Therefore, in this area the bed scoring occurs.

3.4 Significance of pressure distribution

Figure 15 shows the depth-averaged velocity vectors below the flood channel height for Case 5 by model II with the assumption of hydrostatic pressure distribution. This indicates that the flow is concentrated and accelerated considerably at the inflection point. As shown in Figure 16, the flow concentration at this point causes an extensive scouring and a wider region of deposition on the opposite bank, and a larger scouring depth causes the flow to concentrate even more. Such a bed variation could not be observed in the results of experiments.

This area of flow concentration exists where the assumption of hydrostatic pressure does not hold well in the case of large relative depth, as shown in Figures 12. Therefore, it is necessary to calculate the flow field and the bed variation in the large relative depth without assuming hydrostatic pressure.

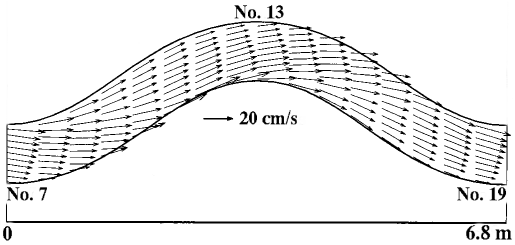

Figure 15: Calculated vector of depth-averaged velocity below flood channel height in Case 5 by model II (Hydrostatic pressure model).

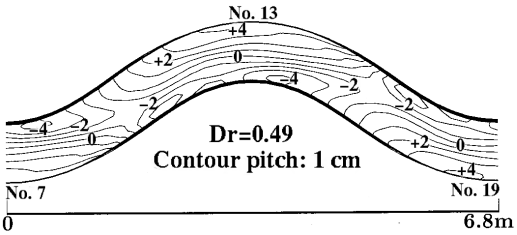

Figure 16: Bed variation contour in Case 5. (Calculated results by model II)

4 CONCLUSIONS

The following was obtained by a 3-D numerical analysis of flow and bed deformation in a compound meandering channel.

When the relative depth is low, the characteristics of the flow resemble those of a

single-section meandering channel. For this case, the deviation of pressure intensity from the hydrostatic pressure distribution is relatively small, therefore the hydrostatic approximation is at some degree reasonable. However, when the relative depth is high, the deviation of pressure intensity from hydrostatic pressure distribution is large and the results with the hydrostatic pressure approximation can not represent the observed flow and bed topography in laboratory experiments. For this case therefore the hydrostatic pressure approximation is not suitable.

The numerical analysis has shown the importance of secondary flow structures in the formation of the bed features. When the relative depth is high, the flow from the flood plain enters the main channel producing the secondary flow with an inverse rotation to the one observed in curved channels with single cross sections. This secondary flow goes toward the bed at the inner bank. As results, scoring occurs at the inner bank. On the contrary, deposition occurs at the outer bank.

REFERENCES

Ashida, K., S. Egashira, B. Liu and M. Takiguchi, "Flow characteristics and bed variations in a meandering channel with flood-plains", *Annuals Disaster Prevention Research Institute*, *Kyoto University*, No.32B-2, pp. 527-551, 1989, (in Japanese).

Ashida, K., S. Egashira, and B. Liu, "A study of the hydraulics of meandering compound channel flows", *Proceedings of the Hydraulic Engineering*, *JSCE*, Vol. 34, pp. 397-402, 1990, (in Japanese).

Kinoshita, R., "Experimental study concerning field work of alluvial phenomena at flooding and best possible river course example", *Control of Flood Flows in Fluvial Rivers and Improvement of Safety of River Channel during Flood*, *Report of Scientific Research Fund*, No. A-62-1, pp. 63-168, 1988, (in Japanese).

Mori, A., "Three dimensional analysis of meandering open channel flow, Control of Flood Flows in Fluvial Rivers and Improvement of Safety of River Channel during Flood", *Report of Scientific Research Fund*, *Ministry of Education*, No. A62-1, pp. 91-104, 1986a, (in Japanese).

Mori, A. and T. Kishi, "The characteristics of river bed topography of Ishikari-river observed on the Flood in 1981", *Proc. of the 30th Japanese Conference on Hydraulics*, pp.493-498, 1986b, (in Japanese).

Fukuoka, S., H. Miyazaki, H. Ohgushi, and D. Kamura, "Flow and bed topography in a meandering compound channel with phase difference between the alignment of the main channel and levee", *Annual Journal of Hydraulic Engineering*, *JSCE*, Vol. 40, pp. 941-946, 1996, (in Japanese).

Muto, Y., K. Shiono, H. Imamoto, and T. Ishigaki, "3-Dimensional structure for overbank flow in meandering channel", *Annual Journal of Hydraulic Engineering*, *JSCE*, Vol. 40, pp. 711-716, 1996, (in Japanese).

Fukuoka, S., H. Ogushi, D. Kamura, and S. Hirao, "Hydraulic characteristics of the flood flow in a compound meandering channel Journal of Hydraulic", *Coastal and Environmental Engineering*, *JSCE*, No. 579/II-41, pp. 83-92, 1997a, (in Japanese).

Fukuoka, S., A. Watanabe, D. Kamura, and S. Okada, "Study of rate of bed load and bed topography in a meandering compound channel", *Annual Journal of Hydraulic Engineering*, *JSCE*, Vol. 41, pp. 883-888, 1997b, (in Japanese).

Fukuoka, S., H. Takahashi and D. Kamura, "Compound meandering flow and simple meandering flow in compound meandering rivers-Analysis by the use of aerophotograph flood flow velocity vector", *Annual Journal of Hydraulic Engineering*, *JSCE*, Vol. 41, pp. 971-976, 1997c, (in Japanese).

Jin, H.S., S. Egashira, and B.Y. Liu, "Charac-teristics of meandering compound channel flow evaluated with two-layered 2-D method", *Annual Journal of Hydraulic Engineering*, *JSCE*, Vol. 40, pp. 717-724, 1996.

Fukuoka, S. and A. Watanabe, "Three dimen-sional analysis on flows in meandering compound channels, Journal of Hydraulic", *Coastal and Environmental Engineering*, No.586/II-42, pp.39-50, 1998,

(in Japanese).
Watanabe, A. and S. Fukuoka, “Three dimen-sional analysis on flows and bed topography in a meandering compound channel, Journal of Hydraulic”, *Annual Journal of Hydraulic Engineering*, *JSCE*, Vol. 43, pp. 665-670, 1999, (in Japanese).
Fukuoka, S., A. Watanabe, Y. Kayaba and H. Soda, “Flow and bed profiles in curved channels with discontinuously installed vanes”, *Journal of Hydraulic, Coastal and environmental Engineering*, *JSCE*, No. 479/II-25, pp.61-70, 1993, (in Japanese).
Fukuoka, S. and M. Yamasaka, ”Alternating bars in a straight channel”, *Proc. of the 27th Japanese Conference on Hydraulics*, pp. 703-708, 1983, (in Japanese).